ULTRASOUND IMAGE DE-NOISING THROUGH KARHUNEN-LOEVE (K-L) TRANSFORM WITH OVERLAPPING SEGMENTS

Jawad F. Al-Asad, (Telephone: 773 6930365, Email:jfalasad@uwm.edu)
Alireza Moghadamjoo, (Telephone: 414 2295262, Email:reza@uwm.edu)
Leslie Ying, (Telephone: 414 2295907, Email:leiying@uwm.edu)

Department of Electrical Engineering and Computer Science. University of Wisconsin-Milwaukee USA

ABSTRACT

A new approach to filter out multiplicative noise from ultrasound images is presented in this paper. The noisy image is segmented into small segments, and the global covariance matrix is found. A projection matrix is formed by selecting the maximum eigenvectors of the global covariance matrix. This projection matrix is then used to filter noise by projecting the segment into the signal subspace. This approach is based on the fact that signal and noise are independent (orthogonal) and the signal subspace is spanned by a subset of the eigenvectors corresponding to the set of largest eigenvalues. When applied on simulated and real ultrasound images, our approach has outperformed popular nonlinear de-noising techniques, such as Wavelets, Total Variation Filtering and Anisotropic Diffusion Filtering. It also showed less sensitivity to outliers resulted from the log transformation of the multiplicative noise.

Index Terms— Ultrasound (US) image, Eigenvectors, Eigenvalues, Covariance Matrix, Projection Matrix.

1. INTRODUCTION

Ultrasound medical imaging is considered to be practically harmless to the human body and cost effective. Unfortunately, quality of medical ultrasound image is highly degraded by the presence of the speckle noise.

Speckle noise can be fully developed in ultrasound images when the number of scatterers per resolution cell is large. In this case, it is modeled using a Rayleigh distribution. When the speckle is not fully developed, it is modeled by other models such as Rician and K-distributions, noting that Rician and Rayleigh distributions are special cases of the K-distribution [1].

In literature, speckle noise reduction methods are based on averaging filters and adaptive weighted median filters [2] which can effectively suppress speckle noise, however, they fail to preserve many useful details.

The multiplicative nature of the speckle noise formation was used in [3] in which the author proposes to convert the multiplicative speckle noise into an additive noise by applying the logarithmic transformation to a speckle-noisy image. Subsequently, Wiener filtering is used in order to reject the resultant additive noise, followed by the exponential transformation.

Wavelet transform has been recognized as a powerful tool for recovering signals from noisy data. Methods based on multiscale decompositions [4] consist of three main steps: First, the raw data are analyzed by means of the wavelet transform, then the empirical wavelet coefficients are shrunk, and finally, the de-noised signal is synthesized from the processed wavelet coefficients through the inverse wavelet transform. These methods are generally referred to as *wavelet shrinkage techniques* [5], which are based on a logarithmic transformation to separate the noise from the original image.

A similar approach applied to synthetic aperture radar (SAR) images is presented in [6], where the wavelet-based approach is found among the best approaches for speckle noise removal.

The application of wavelet de-noising to the despeckling problem in medical ultrasound imaging was reported in [4]. The methods, which are based on a multiplicative model of the speckle noise and use the logarithmic transformation to convert the multiplicative noise into an additive one, followed by wavelet de-noising, are referred to as the Homomorphic Wavelet Despeckling (HWDS) methods [7].

It has been reported in [8] that the log transformed multiplicative noise is spiky in nature and follows Fisher-Tippett distribution. The authors have proposed a preprocessing outlier shrinkage stage to Gaussianize the log transformed noise prior to de-noising. In [9] another preprocessing stage, "Adaptive Decorrelation" has been added before the outlier shrinkage stage and resulted in image enhancement.

With our agreement of the spiky nature of the log transformed noise, we believe that different despeckling techniques have different sensitivities to such spikes and outliers. Our aim is to compare the performance of our approach against other approaches without any extra preprocessing added to them. Through the numerical results and visual appearance, we can state that our method can be among the least sensitive to such outliers, especially when compared to HWDS.

The K-L transform or what is known as Principle Component Analysis (PCA) has been one of the most valuable results from applied linear algebra, [10] and [11]. PCA is used abundantly in all forms of analysis from neuroscience to computer graphics, because it is a simple, non-parametric method of extracting relevant informalities from confusing data sets.

In this paper the Karhunen-Loeve (K-L) Transform is implemented through overlapped segments. After the log transformation, the noisy image is segmented into small blocks of $q \times p$ size. The global covariance matrix is formed by averaging the corresponding covariances of the blocks. A projection matrix is calculated by selecting the maximum eigenvectors of the global covariance matrix. This projection matrix is then used to filter the speckle noise by projecting the block into the signal subspace.

This paper is organized as follows: section 2 presents the adopted signal model. The procedure to filter out the speckle noise is presented in section 3. Section 4 summarizes the experimental results of our algorithm when applied on a phantom image and on a real ultrasound image. The paper is concluded in section 5.

2. ULTRASOUND SIGNAL MODEL

A generalized model of a speckled image as proposed in [3] is given by:

$$g(n,m) = f(n,m)u(n,m) + \xi(n,m) \quad (1)$$

where g, f, u, and ξ stand for the observed envelope image, original image, multiplicative and additive components of the speckle noise, respectively. Here the indices n and m denote the axial and lateral indices of the image samples (or, alternatively, the angular and range indices for sector images).

The model in (1) has been successfully used both in ultrasound and SAR imaging. When applied to ultrasound images, model (1) can be considerably simplified by disregarding the additive noise term. This leads to the following simplified model:

$$g(n,m) \approx f(n,m)u(n,m) \quad (2)$$

An alternative model proposed in [2] describes the speckle noise as an additive noise, whose amplitude is proportional to the square root of the true image. This model is given by

$$y = x + u\sqrt{x} \quad (3)$$

where y represents the observed signal, x the noise free signal and u the noise (independent of y, with mean 0). However, this model was proposed to account for the speckle pattern, as it appears on "screen", rather than the envelope detected echo signal. Consequently, adopting the model in (2) as the basic model, it is assumed that the image $g(n,m)$ is observed before the system processing is applied [8].

3. PROPOSED ALGORITHM

In our implementation of the concept of the K-L transform in de-noising a speckle noisy ultrasound image, we avoided subtracting the mean before processing and adding it after processing. Through our experiments we found subtracting the mean can be beneficial for additive noise rather than a log transformed multiplicative noise.

The non-linear logarithmic transformation, for conversion of the multiplicative noise into additive noise, was done globally at the beginning rather than for each segment (block). Doing such a transformation for individual segments is found less efficient.

The following algorithm summarizes the steps of implementing the concept of PCA in de-noising speckle noisy ultrasound images.

Given $n \times m$ speckle noisy ultrasound image.

Step1: Apply logarithmic transformation on the given image.

Step2: Segment the image into overlapping segments (s_i) each of $q \times p$ size, where i is the index of the segment.

Step3: Reshape the $q \times p$ segment (s_i) into $q.p \times 1$ size and find the segment's covariance matrix c_i of the segment s_i, such that $c_i = s_i \times s_i^T$, where T denotes transposition.

Step4: Add up all the (c_i s) and average them by the number of segments of the image to get the overall covariance matrix R. The size of R is $q.p \times q.p$. Since speckle noise development in the ultrasound image varies, this method of averaging all covariances of the blocks serves to connect various speckle distributions within the image, thus yielding better estimation of the global covariance matrix.

Step5: Calculate the eignevalues and eigenvectors of R. Select $k < q.p$ eigenvectors that correspond to the set of largest eigenvalues. Sort the k selected eigenvectors according to their corresponding eigenvalues in descending order, such as the first column of this *feature vector* (F) is the eigenvector that corresponds to the largest eigenvalue. The feature vector (F) size is now $q.p \times k$.

Step7: Calculate the transformation matrix P of size $q.p \times q.p$ such that $P = F \times F^T$, P in this case, is the global projection or transformation matrix.

Step8: Refer back to every reshaped ($q.p \times 1$) overlapping segment and project it by P to get the de-noised segment d such that $d_i = P \times s_i$, the size of d_i is now $q.p \times 1$.

Step9: Reshape the de-noised segment d_i back to the $q \times p$ size. Reconstruct the image by adding up all the updates for all overlapping segments and then average each sample by the number of updates. Fig.1 displays the 2D updates for a 16×16 sized image restructured of 4×4 block segments.

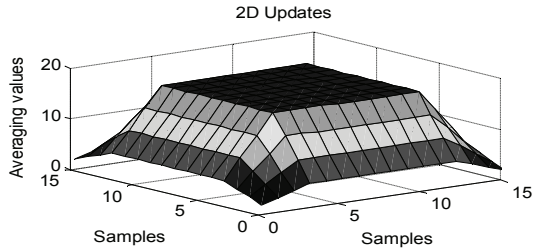

Fig. 1. Blocks of updates

In case of de-noising 1D signals, the principle is the same except vector segments instead of block segments are used and the total added samples are averaged over 1D updates.

4. RESULTS

4.1 In Silico Experiment

To simulate the speckle noise appearance on the screen we have subjected a map image to the "Field II Program". Since every RF echo will be corrupted by a speckle noise depending on the region it penetrates [12], we have independently corrupted the pure RF echoes using multiplicative noise.

The image shown in Fig. 2-a consists of 128 RF-lines penetrating 5625 scatterers per cm^2 of a map image with a lateral resolution of 0.156 *mm*. To test de-noising efficiency, we included sharp edges and curves within the image, as well as, low scattering (represented by the dark areas), high scattering (represented by white areas) and medium scattering (represented by the surrounding). The image is decimated from 1024×128 to yield 256×128. Fig. 2-b shows the corresponding speckle noisy version of the pure image, where the vertical lines appearing in the

image are the result of decimation that has the advantage of removing parts of the noise.

To assess the ability of de-noising, five measuring tools were used: Signal to Noise Ratio (SNR), Speckle Signal to Noise Ratio (S-SNR), Peak Signal to Noise Ratio (PSNR), Signal to Mean Square Error (S-MSE), and to assess the ability of preserving sharp details of the images, *Beta* (β) indicator is used [13]. The closer the index β is to 1, the better the despeckling ability is to preserve the image edges.

Our approach through PCA is compared with nonlinear despeckling schemes. For HWDS, we have used the WaveLab® package (Department of Statistics, Stanford University (http://www-stat.stanford.edu/~wavelab/). Four-level wavelet decomposition and Daubechies with four vanishing moments were used. Since our objective in this paper is not to compare various thresholding schemes, the original approach in [14] is used. The noise variance is estimated by assuming that most empirical wavelet coefficients at the finest level of decomposition are induced by the noise.

Total-Variation Filtering (TVF) which is useful for recovering constant signals, originally described in [15] was used with the best parameters suitable for our case to yield the best visual results and to avoid image blurring; these parameters are 100 iterations with $\lambda = 400$.

Anisotropic Diffusion Filtering (ADF) described in [16] was also set to yield best visual results and to avoid image blurring. ADF has attracted the attention due to its ability of preserving edges while exhibiting numerical stability. It is used with 35 iterations and a conduction coefficient of 25. Speed of diffusion controlled by lambda was set to the maximum ($\lambda = 0.25$). The option of favoring wide regions over smaller ones was chosen for the ADF.

Our proposed approach is used with (16/8-1) denoting a segment size of 16×8 and one eigenvector.

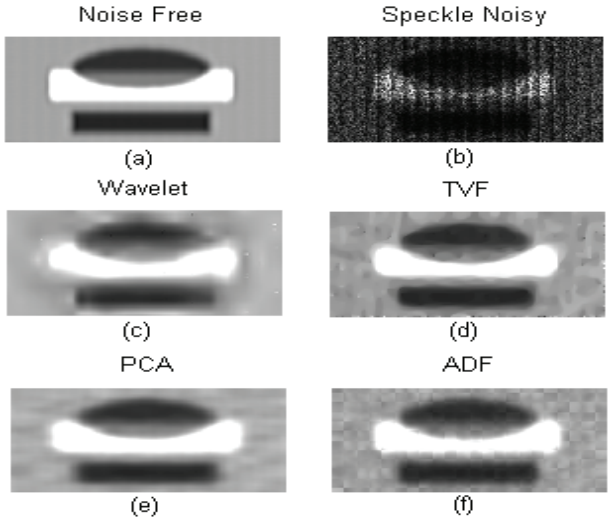

Fig. 2. Visual performance of de-noising schemes

Table 1 lists a numerical comparison as an average of 100 runs for the 256×128 image size shown in Fig. 2-b. Fig. 2 also shows a visual comparison between the de-noising techniques given in Fig. 2-c,d,e and f. Through Table 1 and Fig.2-e, the ability of the proposed approach is clear in maximum cleaning of speckle noise and in preserving the edges.

TABLE 1
NUMERICAL PERFORMANCES OF DE-NOISING SCHEMES FOR 256×128 IMAGE SIZE.

	S-SNR	S/MSE dB	SNR dB	PSNR dB	β
Wavelet	2.163	13.079	15.790	22.293	0.075
TVF	1.774	17.460	20.148	26.748	0.124
ADF	1.789	17.396	20.151	26.667	0.204
PCA 16/8-1	1.803	19.427	21.598	28.122	0.266

4.2 In Vivo Experiment

In order to practically assess our de-noising approach, RF data was obtained over the internet for the experimental scanner RASMUS at the time of peak systole from the carotid artery of a healthy 30 year old male. The transducer was a B-K 8812 linear array transducer with 6.2 MHz linear array probe, 40 MHz sampling frequency and 5 MHz center frequency. 64 RF lines with 1024 samples per RF line were decimated to 128×64 image size shown in Fig. 3.

Fig. 3. Ultrasound image at peak systole of carotid artery

Two factors can determine the de-noising performance of our approach: the segment size and the number of eigenvectors per segment. Using different segment sizes with different numbers of eigenvectors will lead to different de-noising efficiencies. Fig. 4 shows the performance of our de-noising approach through PCA, when applied on the image in Fig. 3, using different segment sizes ($q \times p$) and numbers of eigenvectors denoted by (*ev*). Fig. 5 shows a comparative visual performance between our PCA approach, Wavelet, TVF and ADF. Three-level wavelet decomposition and Daubechies with four vanishing moments were used. TVF is used with 100 iterations and $\lambda = 400$. ADF is used with 20 iterations and a conduction coefficient of 25, speed of diffusion controlled by lambda was set to the maximum ($\lambda = 0.25$), the option of favoring wide regions over smaller ones was chosen for the ADF. Our approach is used with the same parameters shown in Fig. 4-a.

Due to the absence of an original image to compare with, we used two measures: firstly the S-SNR used in section 4.1, which is defined as the ratio of the mean to the standard deviation of the image; Secondly, the ratio of the number of pixels of the image autocorrelation function, which exceeds 75% of its maximum value, to the total number of pixels. This later measure which is indicated by *alpha* (α) is mostly used to evaluate the resolution in ultrasound imaging. Table 2 lists the numerical performance corresponding to Fig. 5, where we can see the better performance of our approach when compared to Wavelet filtering, TVF and ADF.

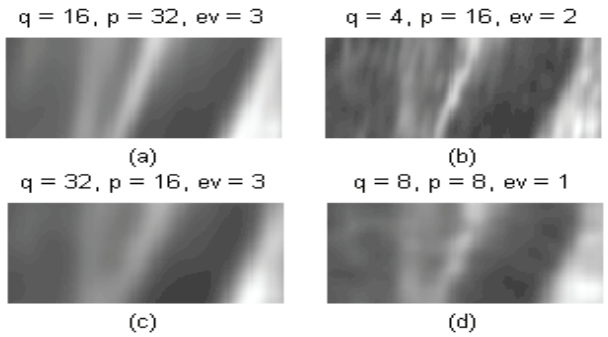

Fig. 4. Visual performance of de-noising through PCA using different $q \times p$ segment sizes and ev eigenvectors

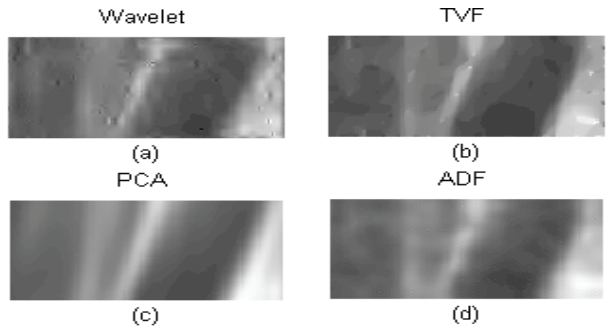

Fig. 5. Visual performance of de-noising techniques

TABLE 2
NUMERICAL PERFORMANCE OF DE-NOISING SCHEMES FOR 128 × 64 IMAGE SIZE SHOWN IN FIG. 5

	Original	Wavelet	TVF	ADF	PCA 16/32-3
S-SNR	0.4915	0.7526	0.6379	0.6363	0.6643
α	0.0006	0.0533	0.0397	0.0631	0.1051

5. CONCLUSIONS

A new approach to filter out multiplicative noise from ultrasound images was presented in this paper. We followed the assumption of linearity to re-express data as a linear combination of its basic components. PCA projections seek to represent the signal in terms of uncorrelated components. Therefore, based on the orthogonality of the noise and signal, discarding the components that correspond to the eigenvectors associated with a subset of the smallest eigenvalues can be thought of as discarding noise from the data.

This implementation of PCA has outperformed most of existing de-noising approaches such as HWDS, TVF and ADF. It has been verified that, per segment size, very few eigenvectors are needed to represent the true signal. It is found that a degree of blur appears in the de-noised image if the difference between the segment size and the number of eigenvectors is very large or when inappropriate segment size is used.

In this paper, we meant to compare our approach with other existing approaches and without using preprocessing stages. Thus the severity of the spiky nature of the log transformed speckle noise can be minimized by a more efficient de-noising technique. This leads to minimizing the overhead and hence the time consumed by many preprocessing stages prior to de-noising.

Our results obtained from real data met our expectation when we applied our algorithm to simulated data. Our approach through overlapped segmentation and hard thresholding the high frequency components while keeping the large magnitude coefficients, deserves future research through other transforms like Short Time Fourier Transform (STFT).

6. REFERENCES

[1] Nikhil Gupta, M. Swamy and E. Plotkin, "Despeckling of medical ultrasound images using data and rate adaptive lossy compression," *IEEE. Trans. On medical imaging*, vol. 24, No.6 .June 2005.

[2] T. Loupas, W. N. Mcdicken, and P. L. Allan, "An adaptive weighted median filter for speckle suppression in medical ultrasonic images," *IEEE Trans. Circuits Syst.*, vol. 36, pp. 129–135, Jan. 1989.

[3] A. K. Jain, "Fundamental of Digital Image Processing," Englewood Cliffs, NJ: Prentice-Hall, 1989.

[4] A. Achim, A. Bezerianos, and P. Tsakalides. "Novel Bayesian multiscale method for speckle removal in medical ultrasound images," *IEEE Trans. Medical imaging,* vol. 20, No. 8, August 2001.

[5] X. Zong, A. F. Laine, and E. A. Geiser, "Speckle reduction and contrast enhancement of echocardiograms via multiscale nonlinear processing," *IEEE Trans. Med. Imag.*, vol. 17, pp. 532–540, Aug. 1998.

[6] L. Gagnon and A. Jouan, "Speckle filtering of SAR images- A comparative study between complex wavelet-based and standard filters," *Wavelet Applications in Signal and Image Processing V, SPIE* Proc. # 3169, pp. 80-91, San Diego, USA, 1997.

[7] S. Gupta, R. C. Chauhan, S. C. Saxena, "Homomorphic wavelet thresholding technique for denoising medical ultrasound images," *Journal of medical engineering and technolog*y, vol. 25, n. 5, pp. 208-214, 2005.

[8] Oleg V. Michailovich and Allen Tannenbaum, "Despeckling of Medical Ultrasound Images" *IEEE Trans. ultrasonics, ferroelectrics, and frequency control*, vol. 53, no. 1, January 2006.

[9] R. K. Mukkavil, J.S. Sahmbi and P. K. Bora, "Modified homomorphic wavelet based despcekling of medical ultrasound images," *CCECE 2008, Canadian conference on electrical and computer engineering,* 2008.

[10] L. David, "Linear Algebra and its Applications," Addison-Wesley, New York. 2000.

[11] J. Shiens, *"*A tutorial on Principle Component Analysis*,"* Institute for Nonlinear Science, University of Carolina, San Diego. La. Jolla, CA 92093 and Systems Neurobiology Laboratories, Sal Institute for Biological Studies. La. Jolla, CA 92037. Dec., 2005.

[12] G. Georgiou. and F. Cohen, "Statistical characterization of diffuse scattering in ultrasound images," *IEEE Trans. On Ultrasonics, Ferroelectrics, and Frequency control*, vol. 45, No. 1, January 1998.

[13] X. Hao, S. Gao, and X. Gao, "A novel multiscale nonlinear thresholding method for ultrasound speckle suppressing," *IEEE Trans. Med. Imag*., vol. 18, pp. 787–794, Sep. 1999.

[14] D. L. Donoho, "De-noising by Soft-Thresholding," *IEEE Trans. Inform. Theory*, vol. 41, pp. 613-627, May 1995.

[15] L. Rudin, S. Osher, and E. Fatemi, "Nonlinear total variation based noise removal algorithms," *Phys. D*, vol. 60, pp. 259–268, 1992.

[16] P. Perona and J. Malik. "Scale-space and edge detection using anisotropic diffusion," *IEEE Trans. on Pattern Analysis and Machine Intelligence*, 12(7):629-639, July 1990.